Celestial Mechanics and Dynamical Astronomy (2005) 92:71–87
DOI 10.1007/s10569-004-3975-7

CHAOTIC DIFFUSION AND EFFECTIVE STABILITY OF JUPITER TROJANS

KLEOMENIS TSIGANIS[1], HARRY VARVOGLIS[2] and RUDOLF DVORAK[3]
[1]*Observatoire de la Côte d' Azur, CNRS, B.P. 4229, 06304 Nice Cedex 4, France, e-mail: tsiganis@obs-nice.fr*
[2]*Department of Physics, Aristotle University of Thessaloniki, 54 124 Thessaloniki, Greece*
[3]*Institut für Astronomie, University of Vienna, A-1180 Vienna, Austria*

(Received: 27 April 2004; revised: 13 September 2004; accepted: 29 September 2004)

Abstract. It has recently been shown that Jupiter Trojans may exhibit chaotic behavior, a fact that has put in question their presumed long term stability. Previous numerical results suggest a slow dispersion of the Trojan swarms, but the extent of the 'effective' stability region in orbital elements space is still an open problem. In this paper, we tackle this problem by means of extensive numerical integrations. First, a set of 3,200 fictitious objects and 667 numbered Trojans is integrated for 4 Myrs and their Lyapunov time, T_L, is estimated. The ones following chaotic orbits are then integrated for 1 Gyr, or until they escape from the Trojan region. The results of these experiments are presented in the form of maps of T_L and the escape time, T_E, in the space of proper elements. An effective stability region for 1 Gyr is defined on these maps, in which chaotic orbits also exist. The distribution of the numbered Trojans follows closely the $T_E = 1$ Gyr level curve, with 86% of the bodies lying inside and 14% outside the stability region. This result is confirmed by a 4.5 Gyr integration of the 246 chaotic numbered Trojans, which showed that 17% of the numbered Trojans are unstable over the age of the solar system. We show that the size distributions of the stable and unstable populations are nearly identical. Thus, the existence of unstable bodies should not be the result of a size-dependent transport mechanism but, rather, the result of chaotic diffusion. Finally, in the large chaotic region that surrounds the stability zone, a statistical correlation between T_L and T_E is found.

Key words: Jupiter Trojans, chaos, 1:1 resonance, effective stability

1. Introduction

Today, almost 100 years since the discovery of (588) *Achilles*, more than 1,200 numbered and multi-oppositioned Trojans are known (see the AstDys database, *hamilton.dm.unipi.it/cgi-bin/astdys/astibo*), orbiting around Jupiter's Lagrangian points. These bodies are in a 1:1 resonance with Jupiter, performing tadpole librations about the stable equilibria of the restricted problem, which are located at a relative mean longitude equal to $\pi/3$ (L_4) or $-\pi/3$ (L_5), with respect to Jupiter. Recently, the stability of these orbits, previously taken for granted, has been put to question.

The numerical results of Milani (1993, 1994) were the first to show that a number of Jupiter Trojans follow chaotic orbits. Although the integration

time was small by today's standards (5 Myrs), these experiments have revealed some possible routes of escape at the borders of the Trojan region, related to secular resonances. Subsequently, Levison et al. (1997) were the first to present numerical results, indicating a slow dispersion of the Trojan swarms, on a time scale shorter than the age of the solar system. In their runs it was shown that the region of effective stability (for 4.5 Gyrs) is smaller than the one found analytically by Rabe (1967). This is in fact the most extensive long-term numerical integration of Trojans to date. The possibility of real Trojans escaping from the swarms in the future, due to the destabilizing effect of the ν_{16} and other high-order secular resonances, was shown by Tsiganis et al. (2000a) and Dvorak and Tsiganis (2000). The role of secular resonances was extensively studied by Marzari and Scholl (2002).

Analytical works on the long periodic motion of the Trojans are numerous and a complete list cannot be presented here. We should point out though that several important papers have been published recently, starting from the work of Érdi (1988, 1997). More refined models on the long periodic libration of the Trojans were published by Namouni and Murray (2000) and Nesvorný et al. (2002). The secular effect of additional perturbing bodies or of an oblate planet were studied by Morais (1999, 2001).

Milani (1993) defined and computed (synthetic) proper elements for the Trojans, which allowed him to search for families. Later, Beaugé and Roig (2001) presented a semi-analytic theory for Trojan proper elements, based on an asymmetric expansion of the disturbing function and on the principle of adiabatic invariance. This work, along with an increased sample of real bodies, allowed them to confirm and improve the results of Milani (1993), concerning the existence of at least two robust families (those of *Menelaus* and *Epeios*, both around L_4).

The first attempt to compute the extent of the stability region for Trojan-type motion was made by Rabe (1967), who studied the linearized equations of motion. Nowadays, there exist more refined analytical techniques, based on the construction of Nekhoroshev-type normal forms. The effective stability region is defined as an open domain of initial conditions around a torus of given frequencies (e.g., in our case the resonant torus corresponding to the Lagrangian points $L_{4,5}$), for which the time, τ, needed to change the actions, J, by a given small amount, say $|J(\tau)-J(0)| \leqslant \varepsilon$, is larger than the age of the solar system. This mathematically well defined and quite elegant approach suffers from the limitations of all strongly constrained theories. From the technical point of view, the 1:1 resonance seems to be even more difficult to tackle, compared to other resonances. Also, the models, in which these techniques are applied, are too simplified, to represent a realistic long-term evolution for Jupiter Trojans. As a result, the width of the stability region found by these methods is typically very small, compared to the one which

can be determined numerically. These points are discussed in detail in Celletti and Giorgilli (1991), Giorgilli and Skokos (1997) and Skokos and Dokoumetzidis (2001).

Since the work of Levison et al. (1997), most numerical work has been oriented towards short-term numerical integrations of large sets of initial conditions, aiming to unveil the resonant structure of the Trojan swarms, and define a stability region in terms of regular/chaotic motion. Important results on this topic have been published by Marzari et al. (2003) and Nesvorný and Dones (2002). However, the most complete work on this subject was presented in this meeting by Robutel et al. (2005) in the same volume. We should also point out the numerical work of Michtchenko et al. (2001), where the important role of the great inequality on Trojan motion was shown, in an indirect way. In that paper it was shown that, if Jupiter and Saturn ever crossed the 5/2 resonance during their early migration, the Trojans would not have survived. Gomes (1998) also studied the effect of planetary migration on Trojans, showing that a near 2/1-resonant configuration for Jupiter and Saturn would also lead to a fast depletion of the swarms.

One has to take care though, since an asteroid undergoing chaotic motion will not necessarily escape from the Trojan region, within the age of the solar system. We remind the reader that ~30% of the main-belt asteroids follow chaotic orbits with Lyapunov times $T_L \leqslant 10^5$ yrs, but many of them have very stable proper elements over Gyr-long time spans. In this paper, we report the results of extensive numerical experiments, performed with the purpose of defining an 'effective stability' region for Trojan-type orbits and comparing with the distribution of real Jupiter Trojans, in orbital elements space. The term 'effective stability' refers not only to regular (quasi-periodic) orbits, but also to chaotic orbits which, however, can wander at the border of the stability region, without escaping within the lifetime of the solar system. The stability region is defined in terms of two quantities, which provide complementary information: (i) the Lyapunov time, T_L, which measures the (inverse of the) local rate of exponential divergence for chaotic orbits, and (ii) the escape time, T_E, which denotes the time needed for a Trojan to encounter Jupiter within a small distance and escape from the tadpole zone.

The structure of this paper is as follows. The way of appropriately selecting initial conditions for the numerical experiment is described in Section 2. The core of our results is given in Section 3, in the form of grey-scale maps, which allow us to define the stability region in the space of proper elements and compare it with the distribution of real Trojans. It is shown that ~14% of the real Trojans are outside the stability region. This result is confirmed by a 4.5 Gyr integration of the 247 real Trojans found on chaotic

orbits with $T_L < 4 \times 10^5$ yrs. By estimating the diameters of the observed bodies, we show that the existence of unstable Trojans cannot be the result of a size-dependent process and that it is most likely the outcome of slow chaotic diffusion. For the chaotic region surrounding the effective stability zone, a power-law statistical correlation between T_L and T_E is found (Section 4). The conclusions of our study and a discussion on open problems are given in Section 5.

2. Numerical Set-up

The physical model we consider consists of the Sun and the four giant planets (Jupiter, Saturn, Uranus and Neptune), fully interacting through Newtonian pointmass gravitational forces. The Trojan (test-particle) is subjected to the forces of the massive bodies. The equations of motion are numerically integrated, using the 2nd order mixed variable symplectic algorithm (MVS) of Wisdom and Holman (1991), as it is implemented in the SWIFT package (Levison and Duncan, 1994). The time step used in our runs was $\delta_t = 0.1$ yrs, i.e., smaller than $0.01 T_J$, where T_J the orbital period of Jupiter. This integration scheme is not appropriate when close encounters between bodies occur. However, in the experiments presented here, we are only interested in calculating the escape time of a Trojan and not in following its subsequent evolution. Thus, as described above, we define the escape time of a Trojan as the time at which it approaches Jupiter within 2 Hill's radii, at which point we stop integrating its orbit.

The initial conditions for the Trojans were selected in such a way so that, for each value of the inclination, i, a 'representative plane' of initial conditions was studied. By this we mean that the initial conditions were chosen as to provide a first approximation to *proper elements*, so that a comparison with the real Trojan population could be made. To do this, we used the model of Érdi (1988) for the long-period motion of a Trojan, in the frame of the elliptic restricted three-body problem, as the basis of our selection.

According to Érdi (1988), the first term in the expansion of the long periodic variations of a Trojan's semi-major axis, a, and relative mean longitude, $\lambda - \lambda'$, is given by

$$\begin{aligned} a - a' &= d_f \sin\theta + O(d_f^2) \\ \lambda - \lambda' &= \pm\pi/3 + D_f \cos\theta + O(D_f^2) \end{aligned} \tag{1}$$

where primed quantities refer to Jupiter. The amplitude of libration in semi-major axis, d_f (in AU), is related to the amplitude of libration, D_f (in radians), of the critical argument, $\sigma = \lambda - \lambda'$, through

$$d_f = \sqrt{3\mu}a' D_f \approx 0.2783 D_f \tag{2}$$

where μ is the ratio of Jupiter's mass to the total mass of the system. In the (σ, a–a') plane, each Trojan orbit has the shape of a topological cycle, centered approximately at the Lagrangian point (at $\pm\ \pi/3$), and the angle θ is the angle between the $a = a'$ axis and the 'position vector' of the Trojan, measured from $\pm\ \pi/3$. During the motion, the angle σ librates approximately between $\pm\ \pi/3$–D_f and $\pm\ \pi/3\ +\ D_f$, while θ circulates. In our experiments, we chose initial conditions around L_4, with $\theta = \pi/2$, i.e., $\sigma = \pi/3$ and $a = a'\ +\ d_f$.

When $a \to a'$ the values of the forced eccentricity and inclination become equal to the (osculating) values of Jupiter's elements. Érdi's model shows that the libration adds only 2nd-order corrections to these values. Then, by selecting the longitude of pericenter of the Trojan, $\bar{\omega}$, and its eccentricity, e, through

$$\begin{aligned} \bar{\omega} &= \bar{\omega}' + \pi/3 \\ e &= e' + e_f \end{aligned} \tag{3}$$

and the longitude of the node, Ω, and inclination, i, through

$$\begin{aligned} \Omega &= \Omega' \\ i &= i' + i_f \end{aligned} \tag{4}$$

the eccentricity offset, e_f, and the inclination offset, i_f, become approximate proper elements, in the framework of the elliptic restricted three-body problem. Hereafter we will refer to the elements e_f, i_f and D_f as eccentricity, inclination and libration width, dropping the subscripts. This choice of initial conditions implies that all test particles have initially a mean anomaly equal to that of Jupiter, $M = M'$.

Following the above described scheme, we constructed four sets of initial conditions, for $0° \le i \le 30°$ with a step of 10°. Each of these sets consisted of 806 orbits, set on a 31×26 grid on the (D, e) plane, with $0 \le e \le 0.25$ and $0° \le D \le 45°$ (the step size being $\delta\mathrm{D} = 1°.5$ and $\delta\mathrm{e} = 0.01$).

Our first numerical experiment consisted in integrating these 3224 orbits for $t_{\mathrm{int}} = 4$ Myrs, along with the variational equations. This time is enough to obtain an estimate of T_{L}, provided that the latter is actually not larger than ~10% t_{int} (see next section). Subsequently we selected only orbits having $T_{\mathrm{L}} < 400{,}000$ yrs to perform our second experiment, which consisted in integrating these new sets of orbits for $t_{\mathrm{int}} = 1$ Gyr.

3. Strong Chaos versus Effective Stability

The solution of the variational equations provides us with a time series for the norm of the deviation vector, $v(t)$, for each orbit. For chaotic orbits this

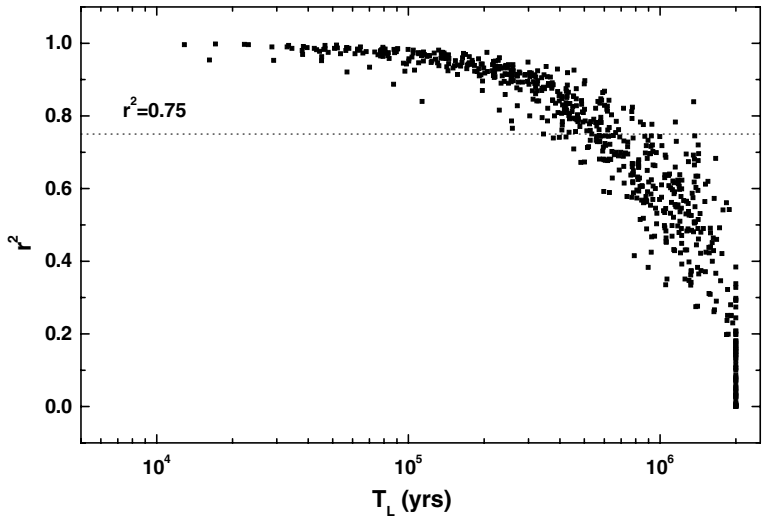

Figure 1. The correlation coefficient of the fit, r^2, as a function of the value of the inverse of the slope, i.e., T_L, for a sample of 667 numbered Trojans. For $T_L > 0.1\ t_{int} \approx$ 400,000 yrs, r^2 drops below 0.75. Had we selected a different value for t_{int}, the functional form would not have changed, but the $r^2 = 0.75$ limit would have shifted towards $0.1\ t_{int}$.

quantity grows exponentially in time, so we can compute the mean growth rate (i.e. a short time approximation of the Lyapunov Characteristic Number), γ, by performing a linear least-squares fit on the $t - \ln[v(t)/v(0)]$ curve. Then, $T_L = 1/\gamma$. This procedure is followed automatically in our code.

It is known, however, that, in order to have an acceptable estimate using this procedure, the integration time should be long enough for γ to have achieved a constant value (see Milani, 1993). A quantitative check of convergence can be made, and its results are shown in Figure 1, for the sample of 667 numbered Trojans found in the catalogue of proper elements, distributed by the AstDys database. The correlation coefficient, r^2, of the fit, used to obtain the slope, is plotted against the inverse of the slope, i.e., T_L. One can immediately realize that the quality of the fit drops as T_L increases. Since we are forced to set a limit as to what we consider as a 'good approximation,' we arbitrarily chose to accept any value of T_L which was obtained by fit, provided that $r^2 \geq 0.75$. Thus, as can be inferred from the plot, for a measurement yielding $T_L >$ 400,000 yrs (i.e. longer than about 1/10 of our integration time span), we cannot decide whether the orbit is mildly chaotic or regular. For this reason, we decided to exclude orbits with $T_L >$ 400,000 yrs from our second experiment of long-term evolution, and concentrate on orbits for which we can claim that they are chaotic, on an acceptable significance level. Concerning our test particle runs, the above described selection method lead us to discard about 25% of them from the

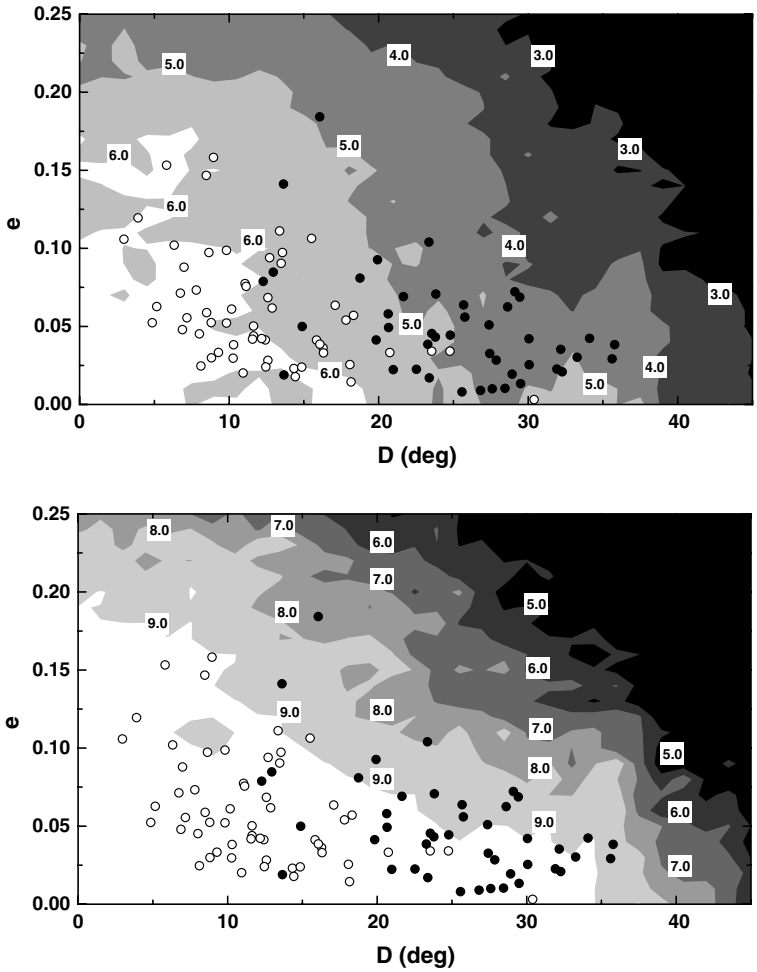

Figure 2. Maps of log T_L (top) and log T_E (bottom) for $i = 0°$. Each grey level corresponds to a change by one order of magnitude. In each panel the real Jupiter Trojans are superimposed, as discussed in the text. The open dots denote the stable Trojans (i.e., $T_L > 400{,}000$ yrs), while the full dots denote the chaotic ones. Note that, in all cases (see also next figures), the distribution of real Trojans follows the shape of the stability zone, but ~14% of the real objects lie outside the $T_E = 1$ Gyr limiting curve.

second experiment. As for the numbered Trojans, 246 bodies (out of 667, i.e. 37%) follow chaotic orbits with $T_L < 400{,}000$ yrs, while the rest could be considered as following stable orbits.

The results of the two runs can be visualized in Figures 2–5. The top panels are grey-scale maps of $\log T_L$, while the bottom panels are grey-scale maps of $\log T_E$, both T_L and T_E measured in years. Each figure corresponds to a different set of initial conditions, i.e., a different initial value of *i*.

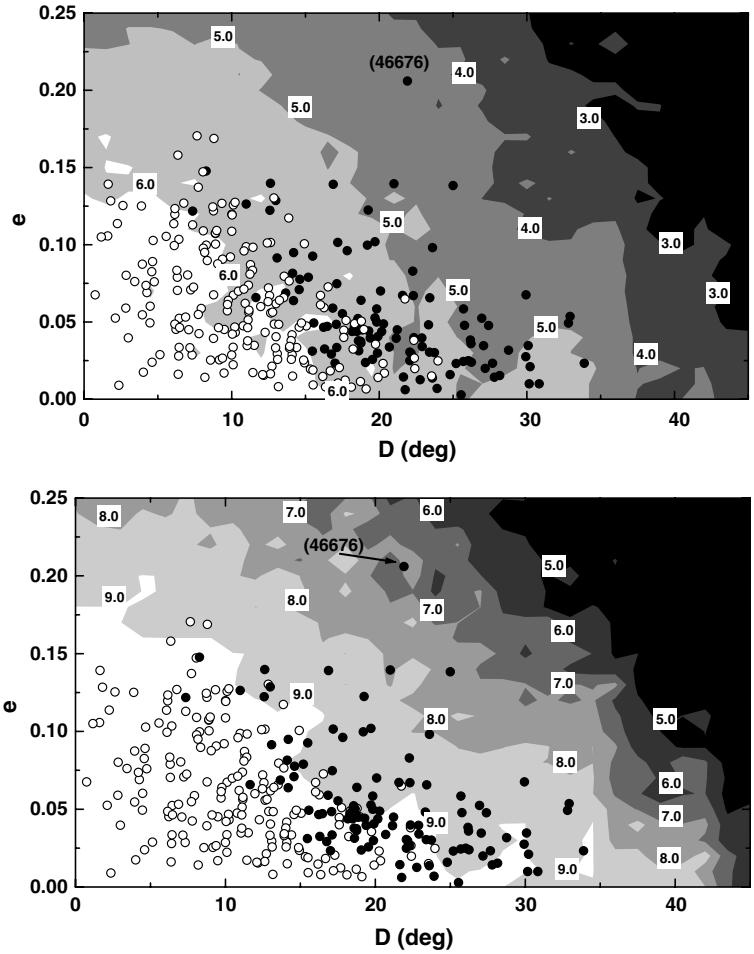

Figure 3. The same as Figure 2, but for $i = 10°$. Also note the existence of real Trojans in highly unstable regions (e.g., object 46676), with $T_L < 10^5$ yrs and $T_E < 10^8$ yrs.

Figure 2 contains the plots for $i_0 = 0°$, Figure 3 for $i_0 = 10°$, Figure 4 for $i_0 = 20°$ and Figure 5 for $i_0 = 30°$. On each panel all numbered Trojans with proper inclination in the range $i_0 - 5° \leq i \leq i_0 + 5°$ are superimposed (obviously, for $i_0 = 0°$, only bodies with $i < 5°$ are shown). The open dots correspond to bodies on regular orbits (i.e., $T_L \geqslant 400{,}000$ yrs), while the full dots correspond to bodies following chaotic orbits. As expected, the chaotic objects are located at greater distances from the nominal location of the Lagrangian point. This projection technique allows us to compare roughly the 1 Gyr effective stability region, defined by the numerical integration of test particles, with the distribution of the real Trojans.

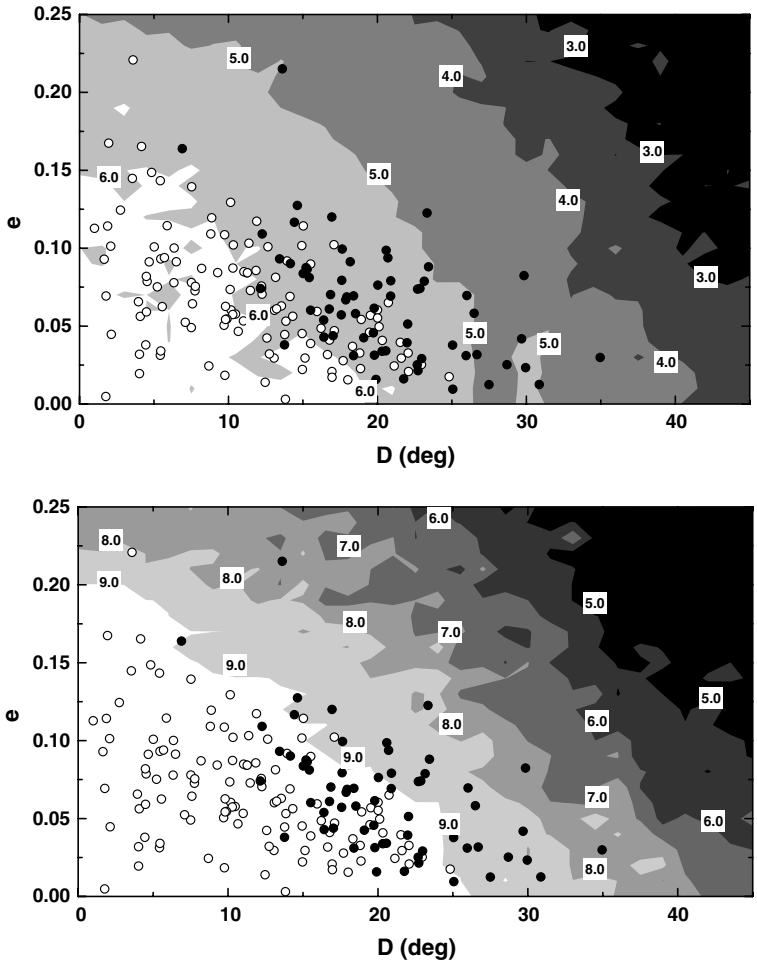

Figure 4. The same as Figure 2, but for $i = 20°$. Note that the extent of the stability region in D shrinks, with respect to the low-inclination cases.

As can be seen in Figures 2–5, ~86% of the real Trojans are projected inside the $T_E \geqslant 10^9$ yrs region, following the shape of the limiting 1 Gyr contour. The remaining 14% (between 12 and 16%, depending on the inclination) is projected outside the stability zone. Note also that ~3% of the real Trojans is projected on highly unstable regions, defined by $T_{\mathrm{L}} \leqslant 10^5$ yrs and $T_{\mathrm{E}} \leqslant 10^8$ yrs. Such an extreme example is asteroid (46676) (see Figure 3). Integrating its nominal orbit we found that it actually escaped from the L_4 region after $T_E = 7.2$ Myrs, a time which agrees well with the location of this object in Figure 3 (the border of the 10^7 yrs contour). The time evolution of its orbital elements is shown in Figure 6. We should note that, a

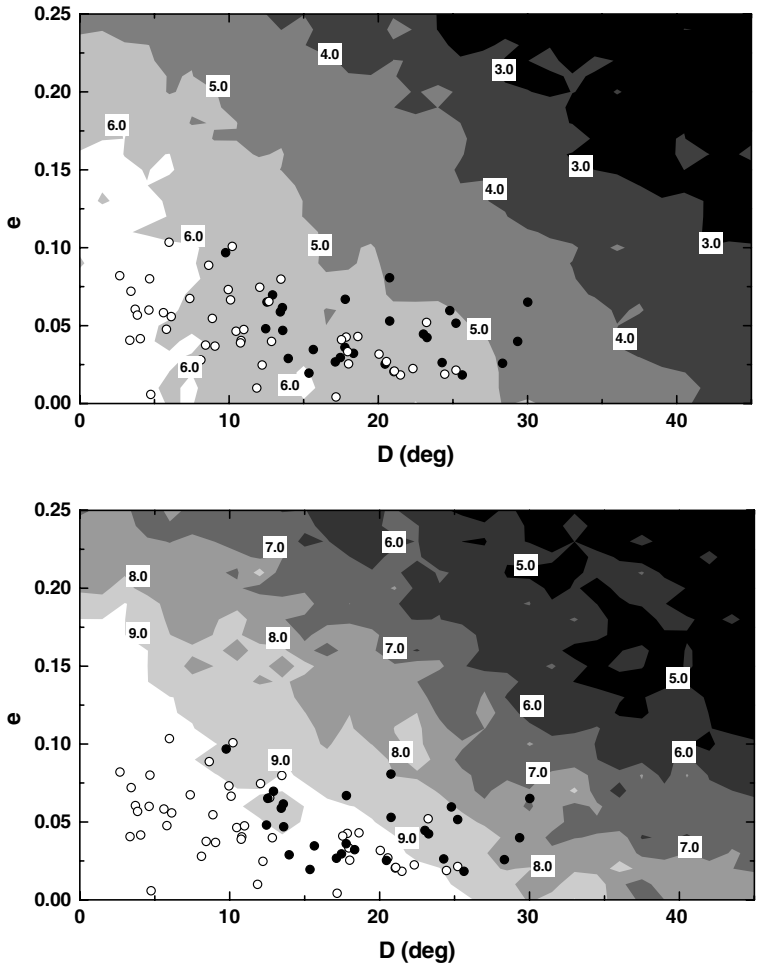

Figure 5. The same as Figure 2, but for $i = 30°$ In this case, $D_{\max} = 25°$, for nearly circular orbits.

significant fraction of chaotic orbits with $T_L < 400{,}000$ yrs, does not escape within 1 Gyr. Thus, our region of effective stability also contains chaotic orbits. The extent of the effective stability region, as given from our results, is comparable to the one calculated by Levison et al. (1997), which is smaller than the one initially calculated by Rabe (1967). However, by integrating a much bigger sample of initial conditions, selected as described in Section 2, we are able to demonstrate for the first time the dependence of the size and shape of the effective stability region on the inclination of the Trojans. As can be seen in the figures, for small values of D, the stability region extends up to $e_{\max} = 0.2$, for any value of i. On the other hand, for nearly circular orbits,

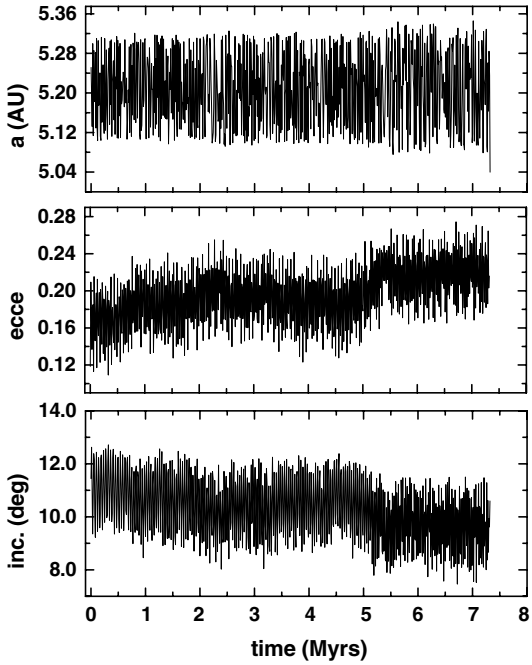

Figure 6. Time evolution of *a, e* and *i* for object (46676). The chaotic evolution of both *e* and *i* is evident. As time progresses, the width of libration in *a* slowly increases, until the asteroid encounters Jupiter.

the stability region shrinks from $D_{\max} = 35°$ to $D_{\max} = 25°$, as i increases from 0° to 30° It is evident from the plots that the distribution of the real Trojans in the (D, e) plane follows the shape of the effective stability region, as the latter is defined for the corresponding value of i.

Based on these results, we could conclude that ~14% of the real Trojans follow orbits which are not stable over the age of the solar system. This of course has to be shown by direct numerical integration of the numbered Trojans. We performed this experiment, setting our integration time to 1 Gyr. Indeed, out of the 246 numbered Trojans with $T_L < 400{,}000$ yrs, 53 escaped within 1 Gyr, i.e.~8% of the total population (667 objects). This number differs from our initial estimate, mainly due to three limiting factors of the above representation: (i) the uncertainty on the approximate proper elements, defined for the test particles, (ii) the projection of the real Trojans on only four planes, with respect to their proper inclination, and (iii) the dependence of the width of the 'actual' effective stability region (for 4.5 Gyrs), on the integration time.

We decided to extend our integration for the chaotic numbered Trojans, going to 4.5 Gyrs. This resulted in 112 chaotic objects, which amounts to

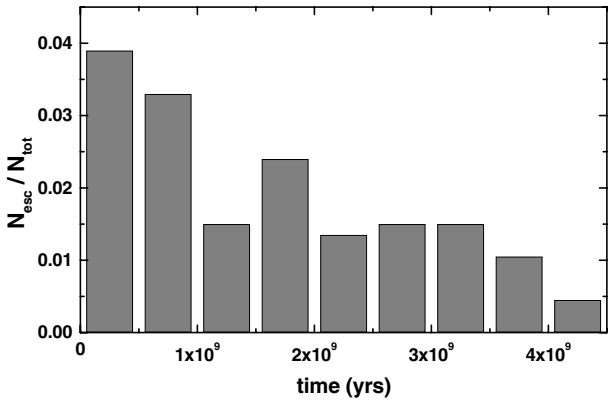

Figure 7. The fraction of escaping Trojans N_{esc}/N_{tot} as a function of time. The size of each bin is 5×10^8 yrs.

17% of the total Trojan population, escaping within the age of the Solar System. The histogram of escape times is shown in Figure 7. One can see that the number of escaping bodies per unit time decays slowly with time. Note also that more than half of the integrated objects follow orbits which, although being chaotic, are stable over the age of the Solar System.

Despite the fact that the existence of unstable Jupiter Trojans has been known for some years, the mechanism by which they may be generated still remains an open issue. There are three main possible mechanisms, one could think of, generating a large fraction of unstable objects: (i) slow chaotic diffusion from the effective stability region, due to secondary resonances (ii) collisions, and (iii) drift due to the Yarkovsky thermal effect (see Farinella and Vokrouhlický, 1999). However, while chaotic diffusion has the same effect no matter what the size of the body is, collisions and thermal forces give size-dependent 'kicks'. Thus, it would be easier for a small body to be transported away from the Lagrangian point (and outside the stability region) by mechanisms (ii) and (iii) than it would be for a large body. Hence, the size distribution of bodies, implanted in the chaotic zone due to mechanisms (ii) or (iii), should be different from the size distribution of regular bodies. In particular, if mechanisms (ii) and (iii) were primarily responsible for replenishing the chaotic region, there should be a lack of large bodies among the currently observed chaotic population.

Using the AstDys catalogue of proper elements, we can derive the size distribution of the Trojans. Fernández et al. (2003) derived the albedo distribution of Jupiter Trojans, showing that it is characterized by a very tight concentration of values around ~0.05. Using this estimate and the values of absolute magnitude, H, reported in the catalogue, an effective diameter, Δ, can be calculated for each body. Then we can derive the distribution of

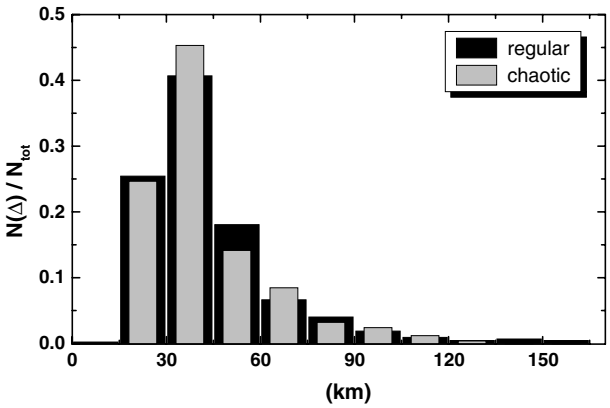

Figure 8. The diameters (Δ) distribution of the regular (black) and chaotic (grey) components of the population of numbered Trojans. The two distributions are normalized with respect to the total number of bodies in each group.

diameters for both the regular and the chaotic population of numbered Trojans. The results are shown in Figure 8. It is evident that the two distributions are nearly identical. This result clearly suggests that the primary mechanism responsible for generating unstable objects is chaotic diffusion through secondary resonances.

It should be noted that the observed Trojans population is only complete up to H ~ 11–12, and thus there are only 4 bodies with $\Delta < 10$ km in the catalogue of numbered Trojans. Future observations may reveal a difference in the small–Δ tails of these two distributions, since $\Delta > 10$ km bodies are very little affected by the Yarkovsky effect over 4 Gyrs, but this is not true for $\Delta \sim 1$ km bodies. However, the important element here is that the probability of finding a body as large as 150 km in diameter is the same, in both the chaotic and the stable region.

4. A Statistical Correlation for Escaping Orbits

Figures 2–5 suggest an approximately smooth decay of both T_L and T_E, as we move away from the origin of each plot, i.e. the nominal location of L_4 at $(D, e) = (0, 0)$. This intriguing result lead us to consider the possible existence of a statistical correlation between these two quantities.

Figure 9 is a log–log plot of T_L versus T_E for each test particle. As before, only orbits with good measurements of T_L ($r^2 > 0.75$) were considered. Both quantities are normalized to the mean revolution period of Jupiter, $T_J \approx 11.86$ yrs. The distribution of points on this plot suggests a power-law

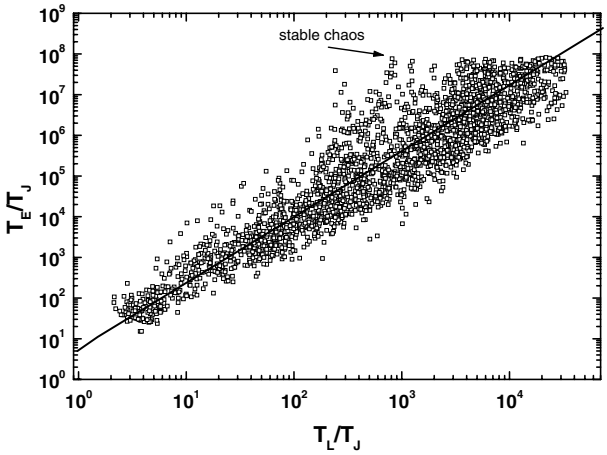

Figure 9. A statistical correlation between T_L and T_E. The least squares line gives the power-law trend. The manifestation of stable chaos, for orbits with $T_L \approx 10^4$ yrs, is indicated by the arrow.

trend, $T_E \approx a\mathrm{T_l}^b$, between these two quantities. Performing a least-squares fit on the data we found $a = 0.75 \pm 0.08$ and $b = 1.62 \pm 0.03$. The correlation coefficient of the fit is $r^2 = 0.88$.

Although the least-squares line seems to fit the data well, it is evident from the plot that the dispersion of the points is quite large, especially when moving towards large values of T_L. Thus, the simple power-law relation described is not useful in determining T_E by computing T_L from a much shorter integration. On the other hand, as shown in Figure 9, there is a well defined lower envelope of the scatter plot. This enables us to make a meaningful extrapolation, which suggests that orbits with $T_L > 650{,}000$ yrs (top-right corner of the plot), although chaotic, would be most likely stable over the age of the solar system.

The scatter of T_E values, around a given value of T_L, increases with T_L, i.e., when approaching the stability region. In Hamiltonian systems, it is known that, as the border of a chaotic region is approached, the geometry of the phase space becomes highly complex, an effect which leads to temporary confinement of chaotic orbits, starting close to the border. Consequently the escape time of such orbits, corresponding to a given narrow range of T_L values, can vary by several orders of magnitude, depending on the duration of the trapping phase. In terms of asteroid dynamics, this is one manifestation of the *stable chaos* phenomenon, first discovered by Milani and Nobili (1992; see also Tsiganis et al., 2000b, 2002a). We remind the reader that stable chaos refers to orbits characterized by a small value of T_L, but of extremely stable orbital elements and a value of T_E typically larger than

$10^4 \cdot T_L$. Such orbits, which are close to the stability boundary, can be seen on the upper part of Figure 7, for $(T_L/T_J) \sim 10^3$.

5. Conclusions and Discussion

In this paper we presented the results of an extensive numerical experiment on Trojan-type motion. A carefully chosen set of 3224 orbits was integrated for 4 Myrs. From this set, all chaotic orbits with $T_L < 400{,}000$ yrs were selected and integrated for 1 Gyr. This experiment took a few months of CPU time on a custom PC. The purpose was to calculate the two relevant quantities, defining the stability region of the 1:1 resonance with Jupiter – the Lyapunov time, T_L, and the escape time, T_E–in a model containing all four giant planets.

The basic results of this experiment are given in Section 3 (Figures 2–8). An effective stability region for 1 Gyr is defined (see Figures 2–5), in the space of proper elements (D, e, i). For nearly circular orbits, the stability region shrinks in D as i increases while, for small values of D, the maximum extent in e is almost constant. As shown in these figures, the distribution of the numbered Jupiter Trojans follows closely the stability curve, for all values of i. However, about ~14% of the real Trojans was found to lie outside the stability region.

A 4.5 Gyr integration of the orbits of 246 chaotic numbered Trojans confirmed the above estimate. Our result is that 17% of the numbered Trojans follows orbits which are unstable over the age of the Solar System. We note that there is another 20% of Trojans undergoing chaotic motion, but whose orbits are stable over 4.5 Gyrs.

The small escape times of many observed Trojans suggest a constant leakage of bodies from the stability region towards the large chaotic sea. However, the mechanism that generates this unstable population was not known up to now. Analyzing the size distribution of the regular and chaotic components of the Trojan population (Figure 8), we can conclude that the main mechanism, by which bodies are delivered from the outshirts of the stability zone to the chaotic region, is independent of the size of the bodies. Thus, chaotic diffusion, rather than collisions or thermal effects, is at the origin of the unstable population.

Chaotic diffusion is the result of higher-order resonant multiplets (either of mean motion or secular type) inside the 1:1 tadpoles region. Robutel et al. (2005) have identified several types of resonances, which cross the stability region. The reader is referred to Figures 1 and 3 of the paper by Robutel et al. (2005) in this volume. The relevance of each of these types of resonance, concerning the transport of bodies, remains to be assessed.

In Section 4 we have found an approximate power-law statistical correlation between the values of T_L and T_E, for chaotic orbits that escape from the 1:1 resonance. A similar result, with b $\approx$ 1.7, was reported by Lecar et al. (1992), for asteroids of the outer main belt. Murray and Holman (1997) have shown analytically that such a relationship exists, in the region where all mean motion resonances of order $q = 1$ overlap. On the other hand, Shevchenko (1998) has shown that a relationship of the form, $T_E \sim {T_L}^2$ can also be found in the immediate vicinity of the border between regular and chaotic motion, around a perturbed principal resonance. It is not easy to give an answer as to which of the two mechanisms we are observing in the case of Trojans. This is obviously related to the study of secondary resonances in the vicinity of the 1:1 resonance, which will be the topic of future work.

Acknowledgements

We would like to thank P. Robutel for the interesting discussions we had, during the 6th Alexander von Humboldt Colloquium. Moreover we would like to thank the referee D. Nesvorný for his constructive criticism and comments which greatly improved the presentation of our work. Part of this work was done during the stay of K.T. in Vienna, and was funded by the Austrian FWF (Project P14375-TPH). K.T. would like to thank the people of the Institute for Astronomy in Vienna for their hospitality. The work of K.T. in O.C.A. is supported by an EC Marie Curie Individual Fellowship, (contract No HPMF-CT-2002-01972).

References

Beaugé, C. and Roig, F.: 2001, 'A semianalytical model for the motion of the Trojan Asteroids: proper elements and families', *Icarus* **153**, 391–415.

Celletti, A. and Giorgilli, A.: 1991, 'On the stability of the Lagrangian points in the spatial restricted problem of three bodies', *Celest. Mech. Dyn. Astr.* **50**, 31–58.

Dvorak, R. and Tsiganis, K.: 2000, 'Why do Trojan ASCs (not) escape?', *Celest. Mech. Dyn. Astr.* **78**, 125–136.

Érdi, B.: 1988, 'Long periodic perturbations of Trojan asteroids', *Celest. Mech.* **43**, 303–308.

Érdi, B.: 1997, 'The Trojan problem', *Celest. Mech. Dyn. Astr.* **65**, 149–164.

Farinella, P. and Vokrouhlický, D.: 1999, 'Semi-major axis mobility of asteroid fragments', *Science* **283**, 1507–1510.

Fernández, Y. R., Sheppard S. S., and Jewitt D.: 2003, 'The Albedo distribution of Jovian Trojan asteroids', *Astron. J.* **126**, 1563–1574.

Giorgilli, A. and Skokos, C.: 1997, 'On the stability of the Trojan asteroids', *Astron. Astrophys.* **317**, 254–261.

Gomes, R. S.: 1998, 'Dynamical effects of planetary migration on primordial Trojan-type asteroids', *Astron. J.* **116**, 2590–2597.

Lecar, M., Franklin, F. and Murison, M.: 1992, 'On predicting long-term orbital instability – A relation between the Lyapunov time and sudden orbital transitions', *Astron. J.* **104**, 1230–1236.

Levison, H. F. and Duncan, M. J.: 1994, 'The long-term dynamical behavior of short-period comets', *Icarus* **108**, 18–36.

Levison, H., Shoemaker, E. M. and Shoemaker, C. S.: 1997, 'The dispersal of the Trojan asteroid swarm', *Nature* **385**, 42–44.

Marzari, F. and Scholl, H.: 2002, 'On the Instability of Jupiter's Trojans', *Icarus* **159**, 328–338.

Marzari, F., Tricarico, P. and Scholl, H.: 2003, 'Stability of Jupiter Trojans investigated using frequency map analysis: the MATROS project', *Mon. Not. R. Astron. Soc.* **345**, 1091–1100.

Milani, A.: 1993, 'The Trojan asteroid belt: proper elements, stability, chaos and families', *Celest. Mech. Dyn. Astron.* **57**, 59–94.

Milani, A.: 1994, The Dynamics of the Trojan Asteroids. IAU Symp. 160: Asteroids, Comets, Meteors, 1993, pp. 159–174.

Milani, A. and Nobili, A. M.: 1992, 'An example of stable chaos in the Solar System', *Nature* **357**, 569–571.

Michtchenko, T. A., Beaugé, C. and Roig, F.: 2001, 'Planetary migration and the effects of mean motion resonances on Jupiter's Trojan asteroids', *Astron. J.* **122**, 3485–3491.

Morais, M. H. M.: 1999, 'A secular theory for Trojan-type motion', *Astron. Astrophys.* **350**, 318–326.

Morais, M. H. M.: 2001, 'Hamiltonian formulation of the secular theory for Trojan-type motion', *Astron. Astrophys.* **369**, 677–689.

Murray, N. and Holman, M.: 1997, 'Diffusive chaos in the outer asteroid belt', *Astron. J.* **114**, 1246–1259.

Namouni, F. and Murray, C. D.: 2000, The effect of eccentricity and inclination on the motion near the Lagrangian points L_4 and L_5; *Celest. Mech. Dyn. Astron.* **76**, 131–138.

Nesvorný, D. and Dones, L.: 2002, How long-lived are the hypothetical Trojan populations of Saturn, Uranus, and Neptune?', *Icarus* **160**, 271–288.

Nesvorný, D., Thomas, F., Ferraz-Mello, S. and Morbidelli A.: 2002, 'A perturbative treatment of the co-orbital motion', *Celest. Mech. Dyn. Astron.* **82**, 323–361.

Rabe, E.: 1967, 'Third-order stability of the long-period Trojan librations', *Astron. J.* **72**, 10–19.

Robutel, P., Gabern, F. and Jorba, A.: 2005, 'The observed Trojans and the global dynamics around the Lagrangian points of the Sun–Jupiter system', *Celest. Mech. Dynam. Astron.* **92**, 55–71.

Shevchenko, I. I.: 1998, 'On the recurrence and Lyapunov time scales of the motion near the chaos border', *Phys. Lett. A* **241**, 53–60.

Skokos, C. and Dokoumetzidis, A.: 2001, 'Effective stability of the Trojan asteroids', *Astron. Astrophys.* **367**, 729–736.

Tsiganis, K., Dvorak, R. and Pilat-Lohinger, E.: 2000a, 'Thersites: a 'jumping' Trojan?', *Astron. Astrophys.* **354**, 1091–1100.

Tsiganis, K., Varvoglis, H. and Hadjidemetriou, J. D.: 2000b, 'Stable chaos in the 12:7 mean motion resonance and its relation to the stickiness effect', *Icarus* **146**, 240–252.

Tsiganis, K., Varvoglis, H. and Hadjidemetriou, J. D.: 2002a. 'Stable chaos in high-order Jovian resonances', *Icarus* **155**, 454–474.

Tsiganis, K., Varvoglis, H. and Hadjidemetriou, J. D.: 2002b, 'Stable chaos versus Kirkwood gaps in the asteroid belt: a comparative study of mean motion resonances', *Icarus* **159**, 284–299.

Wisdom, J. and Holman M.: 1991, 'Symplectic maps for the *n*-body problem', *Astron. J.* **102**, 1528–1538.